Supplementary Information

Two-Dimensional SnS_2 Nanosheets as Electron Transport and Interfacial Layers Enable Efficient Perovskite Solar Cells

Yichuan Rui[a,*], Tianpeng Li[a], Bin Li[a], Yuanqiang Wang[a], Peter Müller-Buschbaum[b,c]

[a]*College of Chemistry and Chemical Engineering, Shanghai University of Engineering Science, Shanghai 201620, P. R. China*

[b]*Lehrstuhl für Funktionelle Materialien, Physik-Department, Technische Universität München, Jams-Franck-Strasse 1, 85748 Garching, Germany*

[c]*Heinz Maier-Leibnitz Zentrum (MLZ), Technische Universität München, Lichtenbergstr. 1, 85748 Garching, Germany*

**E-mail: ryc713@126.com*

1. Characterization

The morphologies of the films and devices were characterized by a field-emission scanning electron microscope (FESEM) (SU8010, Hitachi, Japan) and transmission electron microscope (TEM) (2100F, JEOL, Japan). AFM images were characterized by an atomic force microscope (Dimension, Germany Bruker). X-ray diffraction (XRD) spectra were measured by using a Rigaku D/Max 2550 V X-ray diffractometer with Cu Kα ($\lambda = 0.154$ nm) radiation. The infrared spectra were performed by Fourier transform infrared spectrometer (PerkinElmer, USA). The transmittance and absorption spectra were performed using a Lambda 950UV–vis spectrophotometer (PerkinElmer, USA). X-ray photoelectron spectroscopy (XPS) and Ultraviolet photoelectron spectroscopy (UPS) were measured by an Escalab 250Xi XPS system (Thermo Scientific, USA). Steady-state photo-luminescence (PL) and time-resolved photoluminescence (TRPL) were performed by using a FLS920 transient optical spectrometer (Edinburgh Instruments, UK). The photocurrent density-voltage (J-V) curves were performed by a digital source meter analyzer (Keithley 2400) under AM 1.5G with the light intensity calibrated to 100 mW cm^{-2}. Electrochemical impedance spectroscopy (EIS) was acquired with a Zahner-elecktrik (Germany) workstation. The PSCs were masked using a shadow metal mask to limit the active cell area to 0.16 cm^2.

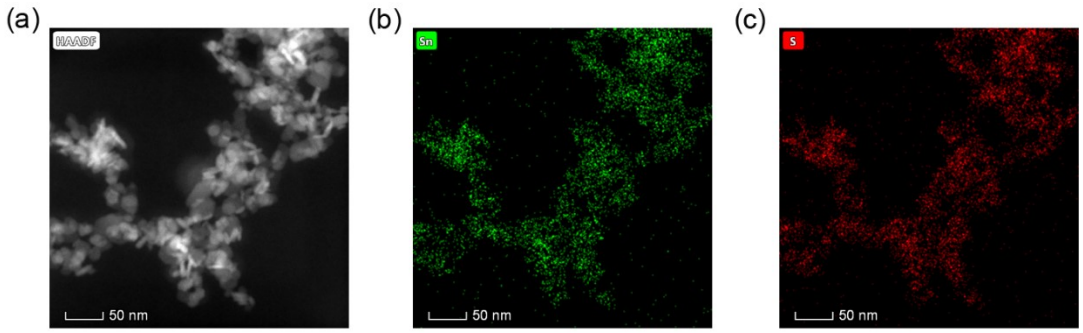

Fig. S1 (a) High-angle annulus dark field TEM image of NS-1 SnS_2 nanosheets, and the EDS mapping of (b) Sn and (c) S elements.

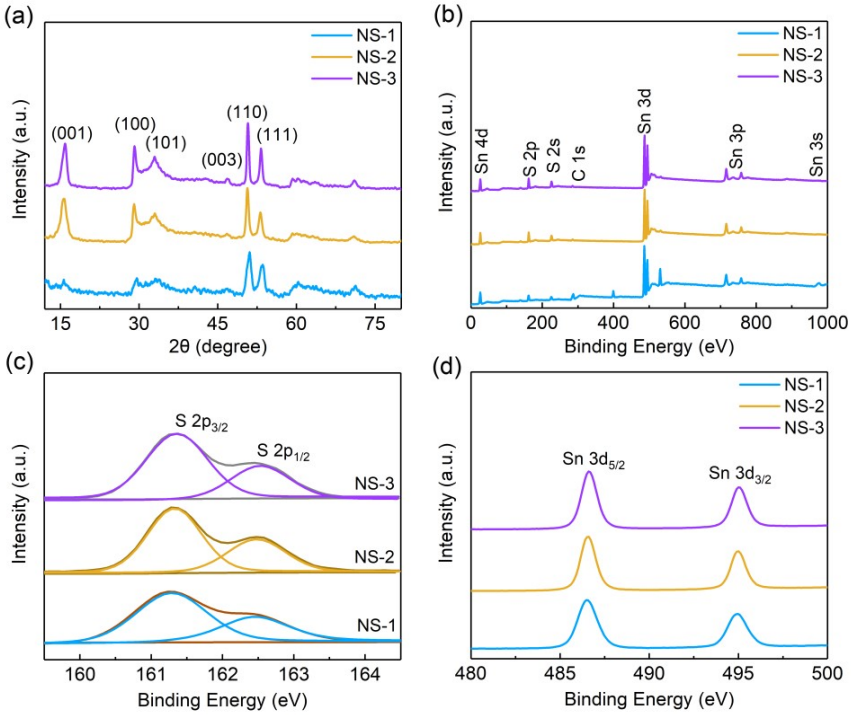

Fig. S2 (a) XRD, (b) XPS survey, (c) S 2p and (d) Sn 3d spectra of the SnS_2 ETLs.

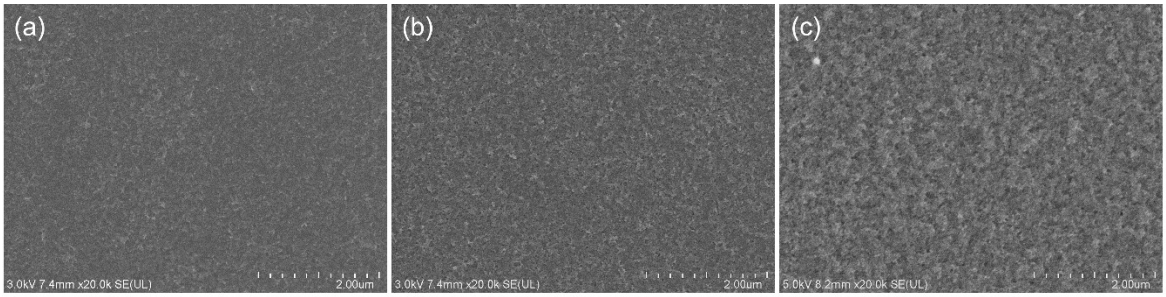

Fig. S3 Top-view SEM images of SnS_2 ETLs: (a) NS-1, (b) NS-2 and (c) NS-3.

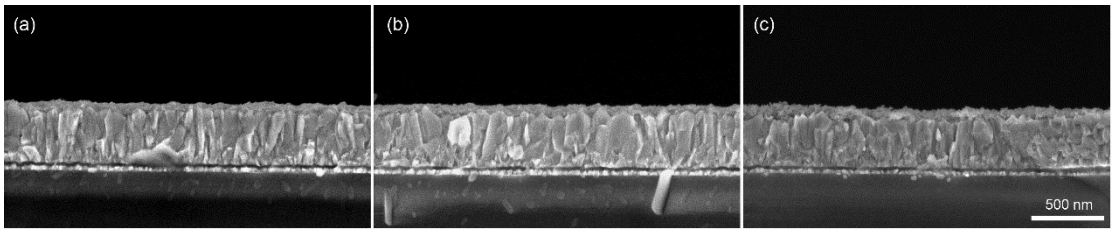

Fig. S4 Cross-sectional SEM images of SnS_2 ETLs: (a) NS-1, (b) NS-2 and (c) NS-3.

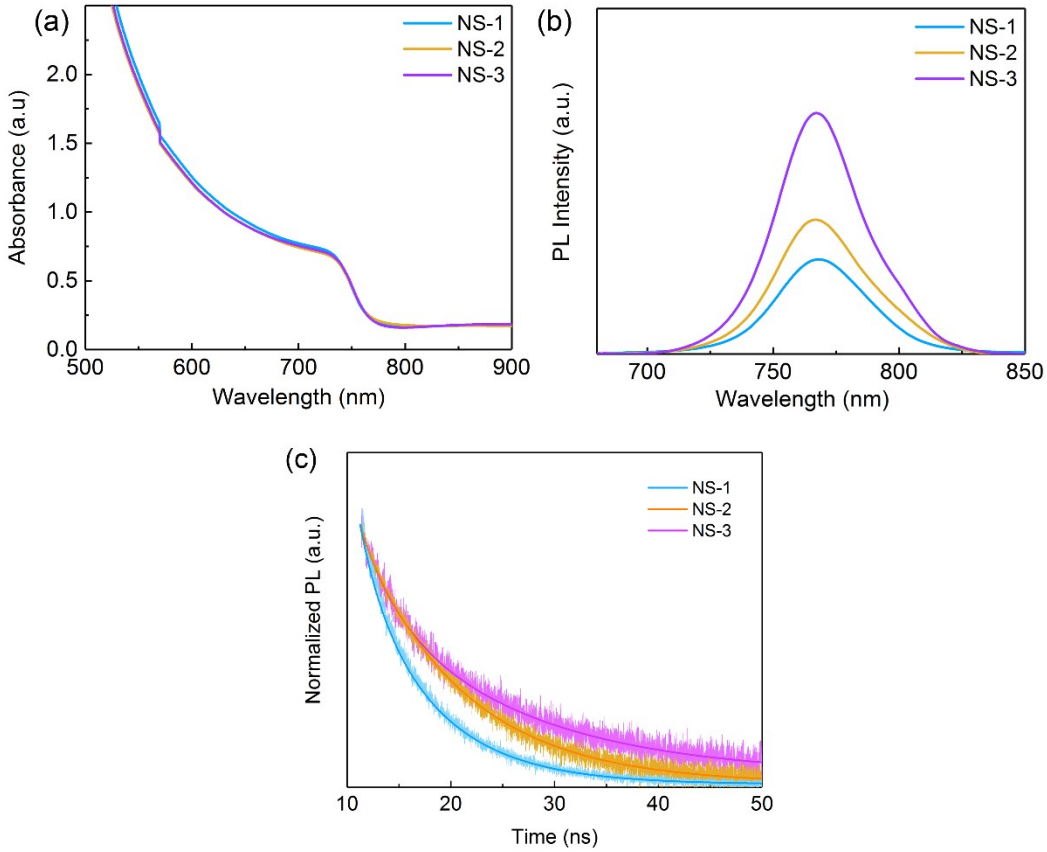

Fig. S5 (a) Absorbance spectra, (b) steady-state PL and (c) TRPL spectra of FTO/NS-1/perovskite, FTO/NS-2/perovskite and FTO/NS-3/perovskite.

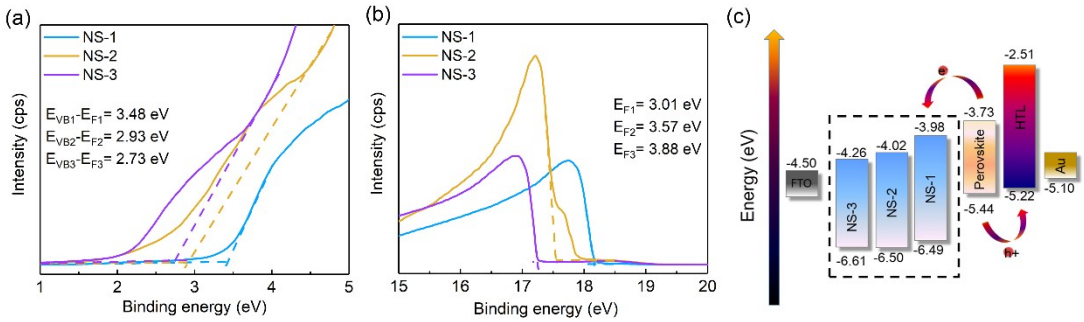

Fig. S6 (a) Valence band region and (b) secondary-electron cut-off of the SnS_2 films. (c) The energy level diagram of the devices.

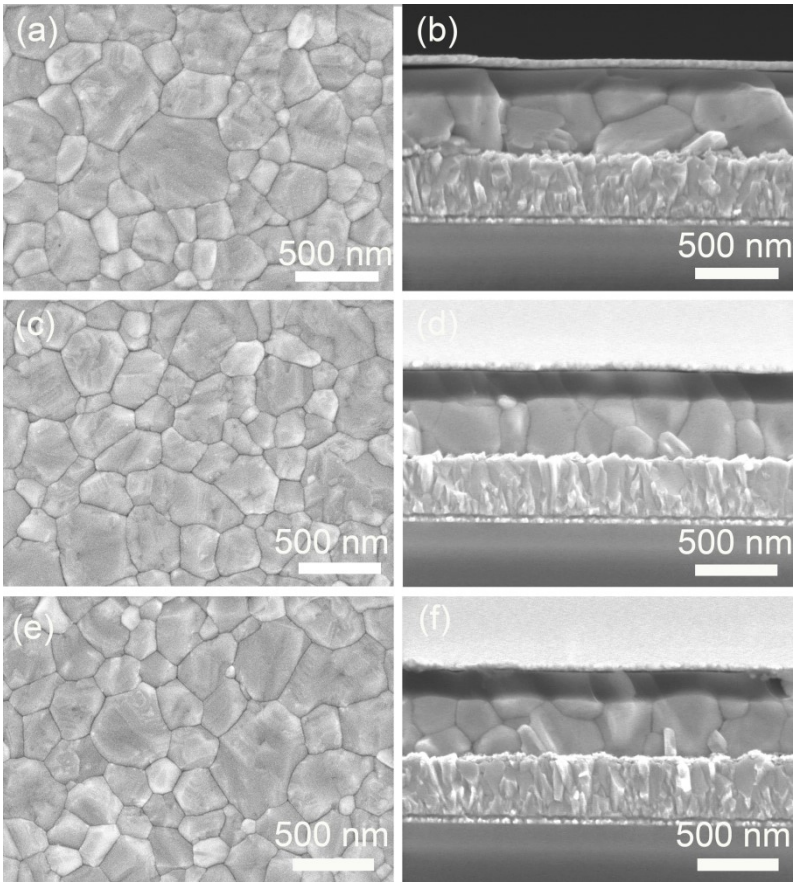

Fig. S7 (a,c,d) Surface and (b,d,f) cross-sectional SEM images of perovskite films based on different ETLs: (a,b) NS-1, (c,d) NS-2, (e,f) NS-3.

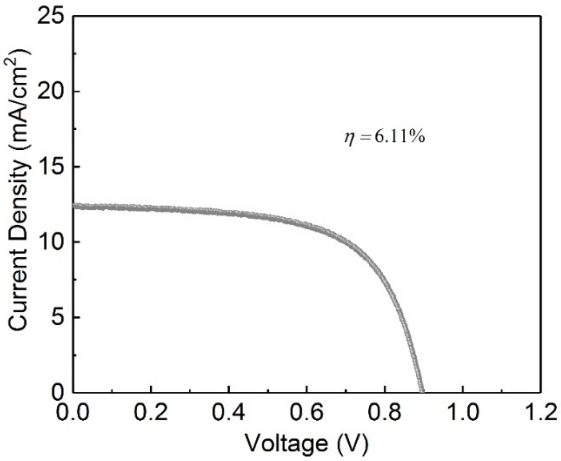

Fig. S8 The J-V curve of PSCs without ETLs.

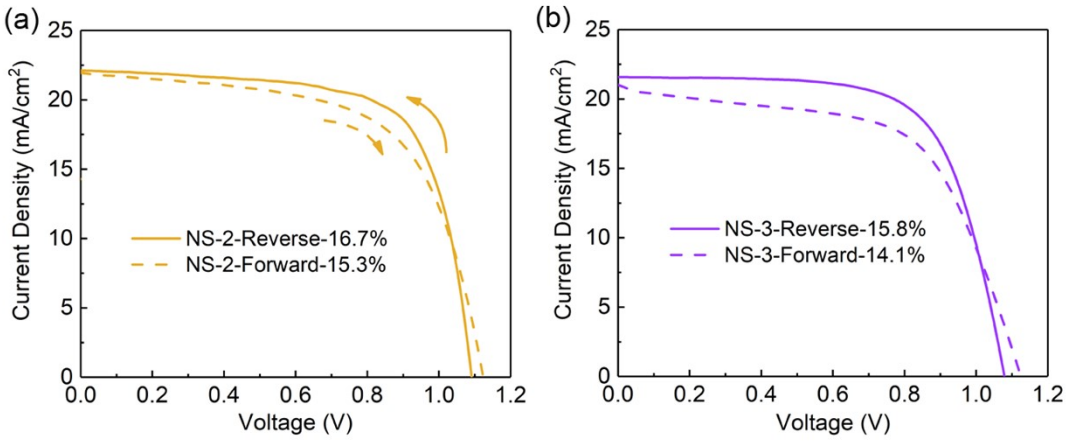

Fig. S9 The J-V curves of (a) NS-2 and (b) NS-3 PSCs under reverse and forward scan.

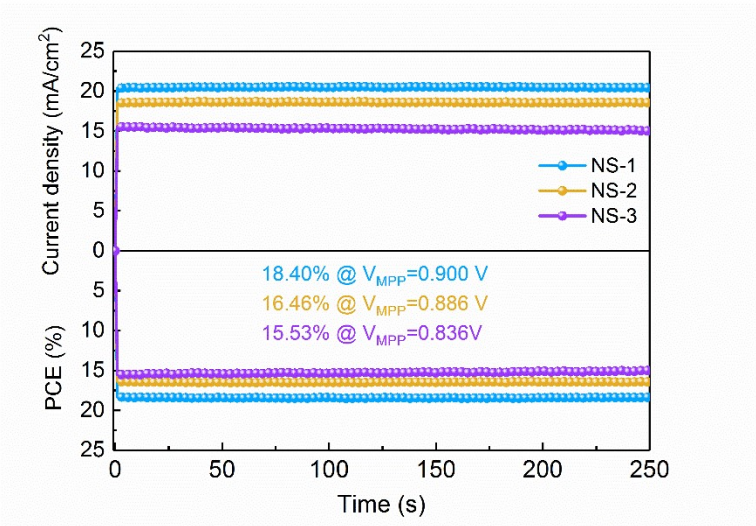

Fig. S10 Stabilized current density and PCE of PSCs at maximum power point.

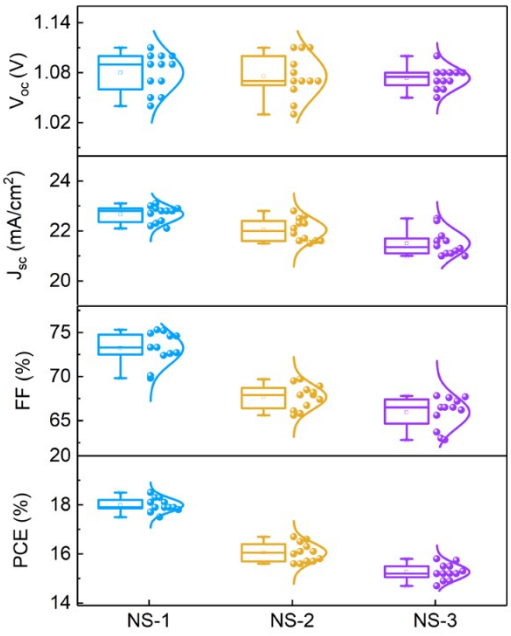

Fig. S11 Statistics of the photovoltaic parameters of the PSCs based on NS-1, NS-2, NS-3.

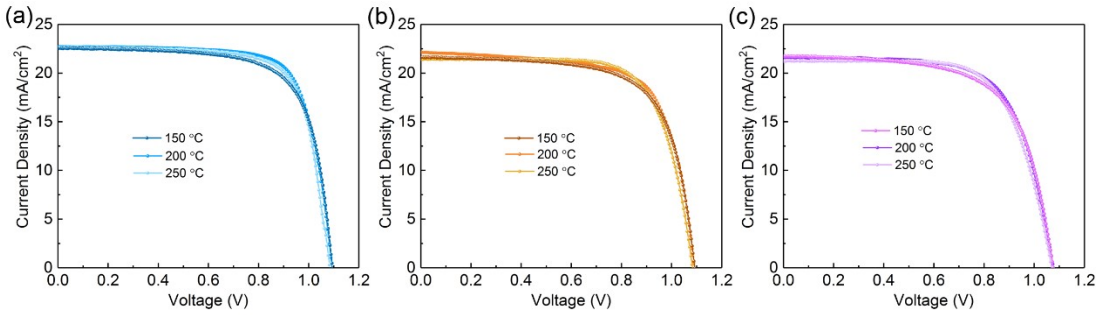

Fig. S12 The J-V curves of PSCs based on different annealing temperature: (a) NS-1, (b)NS-2 and (c) NS-3

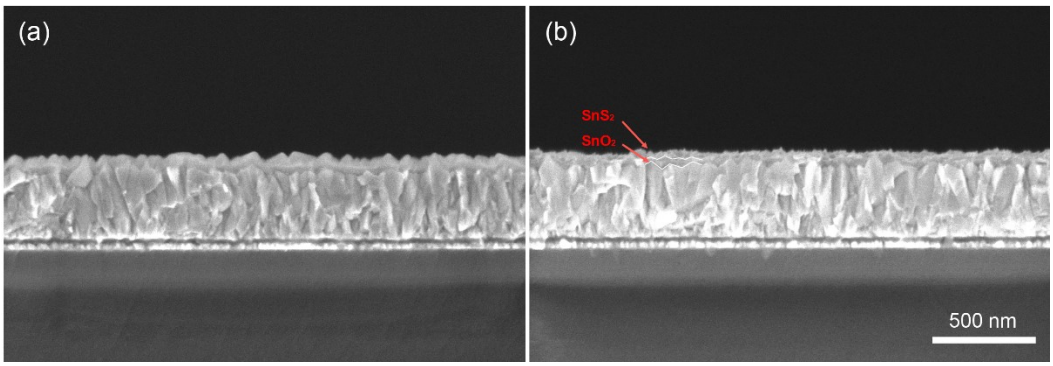

Fig. S13 Cross-sectional SEM images of (a) SnO_2 and (b) SnO_2-SnS_2 ETLs.

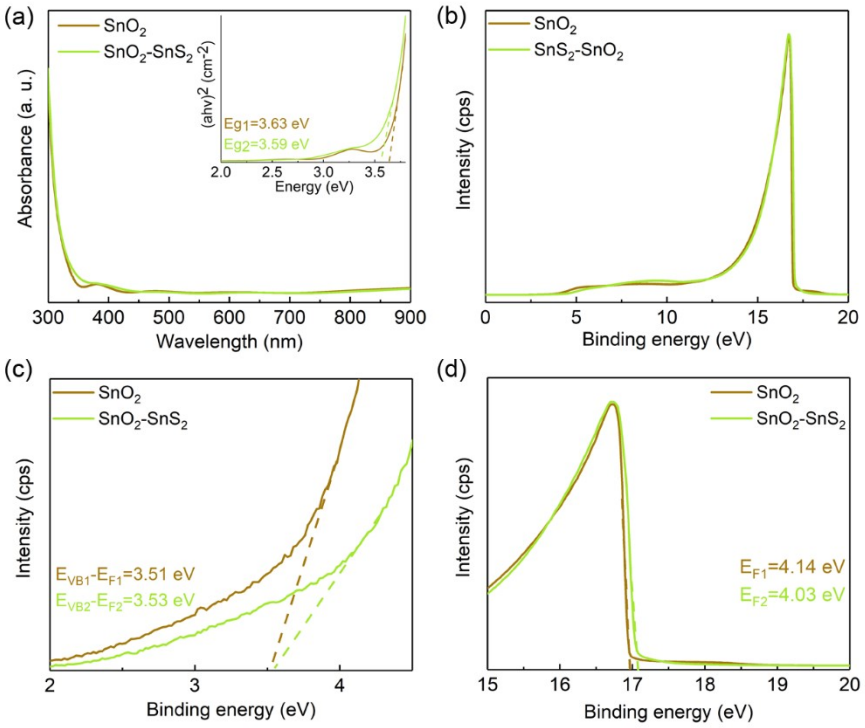

Fig. S14 (a) UV-vis absorbance spectra and the corresponding Tauc plot (inset). (b) UPS spectra. (c) Valence band region and (d) secondary-electron cut-off.

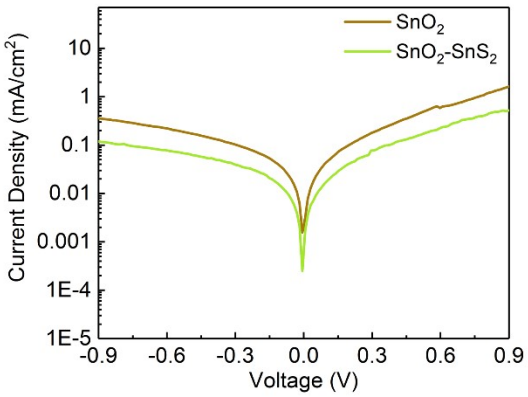

Fig. S15 Dark current-voltage responses of SnO_2 and SnO_2-SnS_2 PSCs.

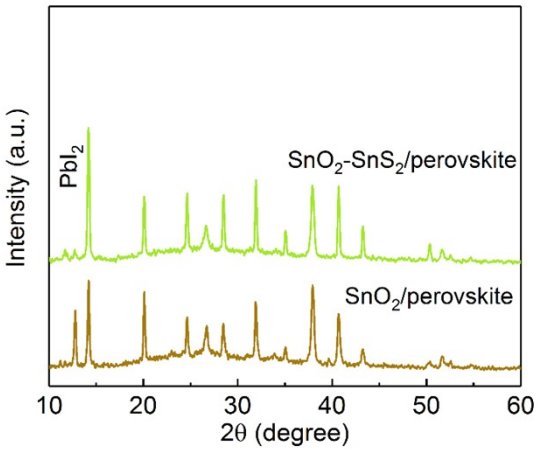

Fig. S16 XRD of perovskites prepared on SnO_2 and SnO_2-SnS_2 ETLs stored in air atmosphere for 14 days (relative humidity 40~50%).

Table S1. Photovoltaic parameters of PSCs based on different annealing temperature.

Samples		V_{oc} (V)	J_{sc} (mA/cm^2)	FF (%)	PCE (%)
NS-1	150 °C	1.09	22.5	71.3	17.6
	200 °C	1.09	22.7	74.9	18.5
	250 °C	1.08	22.6	73.9	18.2
NS-2	150 °C	1.09	21.6	68.7	16.3
	200 °C	1.09	22.1	69.5	16.7
	250 °C	1.08	21.5	71.5	16.6
NS-3	150 °C	1.08	21.7	65.1	15.2
	200 °C	1.08	21.6	67.8	15.8
	250 °C	1.07	21.2	68.5	15.6

Table S2 The trap-filled limit voltage and trap-state density of the devices based on different SnS_2 ETLs.

Sample	NS-1	NS-2	NS-3
V_{TFL} (V)	0.42	0.44	1.24
Trap densities (10^{16} cm^{-3})	0.87	0.91	2.57

Table S3 Fit data from TRPL curves.

Sample	τ_1 (ns)	A_1	τ_2 (ns)	A_2	$\tau_{avg.}$ (ns)
SnO_2/Perovskite	3.73	29.74	19.81	70.26	18.62
SnO_2-SnS_2/Perovskite	1.65	49.64	16.56	50.36	15.23

$\tau_{avg.}$ are calculated by using the equation of $\tau avg. =$

Table S4 Summary of the device performance based on metal sulfide ETLs.

Year	Materials	V_{oc} (V)	J_{sc} (mA/cm^2)	FF (%)	PCE (%)	Ref.
2018	CBD CdS	~0.95	~18.0	~50.0	~10%	[1]
2018	sputtered CdS	1.10	20.71	58.0	13.17%	[2]
2019	MoS_2	0.89	21.7	63.8	12.68%	[3]
2020	2H-TaS_2	0.94	22.5	66.2	14.82%	[4]
2020	2H-WS_2	1.12	22.24	0.731	18.21%	[5]
2018	SnS_2 Arrays	0.95	23.70	66.1	13.63%	[6]
2018	Exploited SnS_2	1.161	23.55	73	20.12%	[7]
2019	Evaporated SnS_2	1.011	21.70	60.0	13.2%	[8]
2020	SnS_2/SnS	1.08	23.27	72.0	18.08%	[9]
2021	TiS_2-TiO_2	1.13	22.4	75.2	18.73%	[10]
this study	SnS_2 nanosheet	1.09	22.7	74.9	18.5%	—
this study	SnO_2-SnS_2	1.14	23.7	79.2	21.5%	—

References

[1] C. D. Wessendorf, J. Hanisch, D. Müller and E. Ahlswede, *Sol. RRL*, 2018, **2**, 1800056.

[2] Y. Guo, J. Jiang, S. Zuo, F. Shi, J. Tao, Z. Hu,X. Hu, G. Hu, P. Yang and J. Chu, *Solar Energy Materials and Solar Cells*, 2018, 1**78**, 186-192.

[3] R. Singh, A. Giri, M. Pal, K. Thiyagarajan, J. Kwak, J. J. Lee, U. Jeong and K.

Cho, *J. Mater. Chem. A*, 2019, **7**, 7151-7158.

[4] M. Afzali, A. Mostafavi and T. Shamspur, *J. Alloys Compd.*, 2020, **817**, 152742.

[5] N. A. Abd Malek, N. Alias, A. A. Umar, X. Zhang, X. G. Li, S. K. M. Saad, N. A. Abdullah, H. J. Zhang, Z. H. Weng, Z. J. Shi, C. Y. Li, M. M. Rosli and Y. Q. Zhan, *Solar RRL*, 2020, **4**, 2000260.

[6] E. L. Zhao, L. G. Gao, S. Z. Yang, L. K. Wang, J. M. Cao and T. L. Ma, *Nano Research*, 2018, **11**, 5913-5923.

[7] X. J. Zhao, S. S. Liu, H. T. Zhang, S. Y. Chang, W. C. Huang, B. W. Zhu, Y. Shen, C. Shen, D. Y. Wang, Y. Yang and M. K. Wang, *Adv. Funct. Mater.*, 2019, **29**, 1805168.

[8] W. J. Chu, X. Li, S. P. Li, J. D. Hou, Q. H. Jiang and J. Y. Yang, *ACS Appl. Energy Mater.*, 2019, **2**, 382-388.

[9] L. Gao, C. Liu, F. Meng, A. Liu, Y. Li, Y. Li, C. Zhang, M. Fan, G. Wei and T. Ma, *ACS Sustainable Chem. Eng.*, 2020, **8**, 9250-9256.

[10] N. Alias, A. A. Umar, N. A. Abd Malek, K. Liu, X. Li, N. A. Abdullah, M. M. Rosli, M. Y. Abd Rahman, Z. Shi, X. Zhang, H. Zhang, F. Liu, J. Wang and Y. Zhan, *ACS Appl. Mater. Interfaces*, 2021, **13**, 3051-3061.